

First Observation of the Key Intermediate in the “Light-Switch” Mechanism of $[\text{Ru}(\text{phen})_2\text{dppz}]^{2+}$

E. J. C. Olson, D. Hu, A. Hörmann, A. M. Jonkman, M. R. Arkin,[†]
E. D. A. Stemp,[†] J. K. Barton,[†] and P. F. Barbara*

Contribution from the Department of Chemistry, University of Minnesota, Minneapolis, Minnesota 55455, and the Division of Chemistry and Chemical Engineering, California Institute of Technology, Pasadena, California 91125

Received April 10, 1997[Ⓢ]

Abstract: $[\text{Ru}(\text{phen})_2\text{dppz}]^{2+}$ (phen = 1,10-phenanthroline, dppz = dipyrrophenazine) and closely related complexes have previously been observed to have an undetectably small quantum yield of photoluminescence in water but a moderate emission yield when bound to DNA. This so-called “light-switch” effect is a critical factor in the utility of these complexes as spectroscopic probes for DNA. Here we describe a detailed investigation of the photophysics of $[\text{Ru}(\text{phen})_2\text{dppz}]^{2+}$ in aqueous solution, and in mixtures of acetonitrile and water, by time-resolved absorption and emission spectroscopies. The emission of the complex in water has been measured for the first time. A prompt initial emission, derived from a metal-to-ligand charge-transfer (MLCT) excited state typical for polypyridyl–ruthenium complexes, is observed along with a delayed emission attributed to a novel MLCT species. The small quantum yield of photoluminescence for $[\text{Ru}(\text{phen})_2\text{dppz}]^{2+}$ in water, and in water/acetonitrile, depends upon efficient formation of a novel MLCT species, followed by its rapid radiationless decay. The MLCT interconversion is assigned to an intramolecular charge-transfer process that is induced by the polarity and proton donating ability of the solvent.

Introduction

The photoluminescence quantum yields of the complexes $[\text{Ru}(\text{phen})_2\text{dppz}]^{2+}$ and $[\text{Ru}(\text{bpy})_2\text{dppz}]^{2+}$ (Figure 1), where phen = 1,10-phenanthroline, dppz = dipyrrophenazine, and bpy = 2,2'-bipyridine, are extraordinarily sensitive to environment.^{1–6} The emission yield has been reported to be undetectably small in water, but moderate in nonaqueous solvents such as acetonitrile and ethanol.^{1–3} Even more importantly, the emission yield is also moderate when the complexes are intercalated in DNA. Thus, when DNA is added to an aqueous solution of the complexes the yield of emission increases dramatically. This has been denoted as the light-switch effect.⁶ The light-switch effect, the strong binding efficiencies of the complexes, and other factors make these complexes important molecular probes for DNA. Various issues regarding these complexes and their derivatives in DNA have been investigated,^{5–20} and in combination with electron acceptors, these complexes have been used

extensively to investigate photoinduced electron transfer in DNA and micellar environments.^{21–28}

Here we focus on the photophysics of these complexes in aqueous solution and introduce the key intermediate necessary to define the mechanism for the light-switch effect. Experimental data are presented primarily for $[\text{Ru}(\text{phen})_2\text{dppz}]^{2+}$, but presumably the results apply by analogy to other compounds in this class. Many aspects of the spectroscopy and photophysics of $[\text{Ru}(\text{phen})_2\text{dppz}]^{2+}$ are analogous to the extensively investigated non-light-switch complex $[\text{Ru}(\text{bpy})_3]^{2+}$ and related compounds.²⁹ Optical excitation of these complexes in the visible prepares a metal-to-ligand charge-transfer (MLCT) state

* Author to whom correspondence should be addressed at the University of Minnesota.

[†] California Institute of Technology.

[Ⓢ] Abstract published in *Advance ACS Abstracts*, November 15, 1997.

(1) Chambron, J.-C.; Sauvage, J.-P.; Amouyal, E.; Koffi, P. *New J. Chem.* **1985**, *9*, 527–529.

(2) Amouyal, E.; Homs, A.; Chambron, J.-C.; Sauvage, J.-P. *J. Chem. Soc., Dalton Trans.* **1990**, *1990*, 1841–1845.

(3) Chambron, J.-C.; Sauvage, J.-P. *Chem. Phys. Lett.* **1991**, *182*, 603–607.

(4) Sabatini, E.; Nikol, H. D.; Gray, H. B.; Anson, F. C. *J. Am. Chem. Soc.* **1996**, *118*, 1158–1163.

(5) Jenkins, Y.; Friedman, A. E.; Turro, N. J.; Barton, J. K. *Biochemistry* **1992**, *31*, 10809–10816.

(6) Friedman, A. E.; Chambron, J.-C.; Sauvage, J.-P.; Turro, N. J.; Barton, J. K. *J. Am. Chem. Soc.* **1990**, *112*, 4960–4962.

(7) Hiort, C.; Lincoln, P.; Nordén, B. *J. Am. Chem. Soc.* **1993**, *115*, 3448–3454.

(8) Haq, I.; Lincoln, P.; Suh, D.; Nordén, B.; Chowdhry, B. Z.; Chaires, J. B. *J. Am. Chem. Soc.* **1995**, *117*, 4788–4796.

(9) Tuite, E.; Lincoln, P.; Nordén, B. *J. Am. Chem. Soc.* **1997**, *119*, 239–240.

(10) Hartshorn, R. M.; Barton, J. K. *J. Am. Chem. Soc.* **1992**, *114*, 5919–5925.

(11) Holmlin, R. E.; Barton, J. K. *Inorg. Chem.* **1995**, *34*, 7–8.

(12) Stoeffler, H. D.; Thornton, N. B.; Temkin, S. L.; Schanze, K. S. *J. Am. Chem. Soc.* **1995**, *117*, 7119–7128.

(13) Schoonover, J. R.; Bates, W. D.; Meyer, T. J. *Inorg. Chem.* **1995**, *34*, 6421–6422.

(14) Coates, C. G.; Jacquet, L.; Mcgarvey, J. J.; Bell, S. E. J.; Alobaidi, A. H. R.; Kelly, J. M. *Chem. Commun.* **1996**, 35–36.

(15) Dupureur, C. M.; Barton, J. K. *J. Am. Chem. Soc.* **1994**, *116*, 10286–10287.

(16) Dupureur, C. M.; Barton, J. K. *Inorg. Chem.* **1997**, *36*, 33–43.

(17) Schoch, T. K.; Hubbard, J. L.; Zoch, C. R.; Yi, G. B.; Sorlie, M. *Inorg. Chem.* **1996**, *35*, 4383–4390.

(18) Gupta, N.; Glover, N.; Neyhart, G. A.; Singh, P.; Thorp, H. H. *Inorg. Chem.* **1993**, *32*, 310–316.

(19) Welch, T. W.; Corbett, A. H.; Thorp, H. H. *J. Phys. Chem.* **1995**, *99*, 11757–11763.

(20) Arounaguir, S.; Maiya, B. G. *Inorg. Chem.* **1996**, *35*, 4267–4270.

(21) Stemp, E. D. A.; Arkin, M. R.; Barton, J. K. *J. Am. Chem. Soc.* **1997**, *119*, 2921–2925.

(22) Arkin, M. R.; Stemp, E. D. A.; Holmlin, R. E.; Barton, J. K.; Hörmann, A.; Olson, E. J. C.; Barbara, P. F. *Science* **1996**, *273*, 475–480.

(23) Murphy, C. J.; Arkin, M. R.; Ghatlia, N. D.; Bossmann, S.; Turro, N. J.; Barton, J. K. *Proc. Natl. Acad. Sci. U.S.A.* **1994**, *91*, 5315–5319.

(24) Murphy, C. J.; Arkin, M. R.; Jenkins, Y.; Ghatlia, N. D.; Bossmann, S.; Turro, N. J.; Barton, J. K. *Science* **1993**, *262*, 1025–1029.

(25) Holmlin, R. E.; Stemp, E. D. A.; Barton, J. K. *J. Am. Chem. Soc.* **1996**, *118*, 5236–5244.

(26) Arkin, M. R.; Stemp, E. D. A.; Turro, C.; Turro, N. J.; Barton, J. K. *J. Am. Chem. Soc.* **1996**, *118*, 2267–2274.

(27) Olson, E. J. C.; Hu, D.; Hörmann, A.; Barbara, P. F. *J. Phys. Chem. B* **1997**, *101*, 299–303.

(28) Lincoln, P.; Tuite, E.; Nordén, B. *J. Am. Chem. Soc.* **1997**, *119*, 1454–1455.

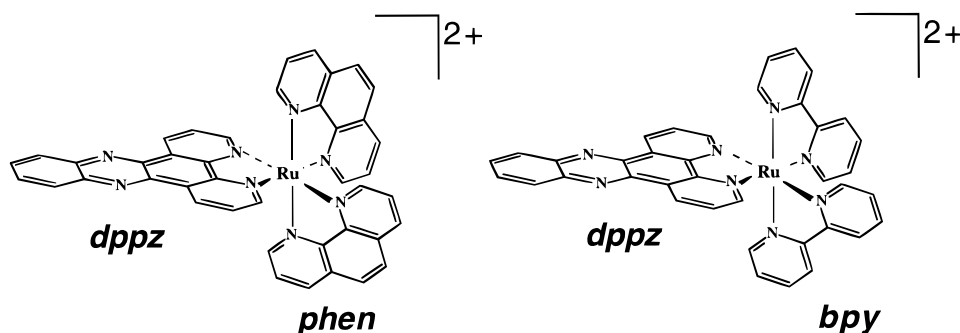
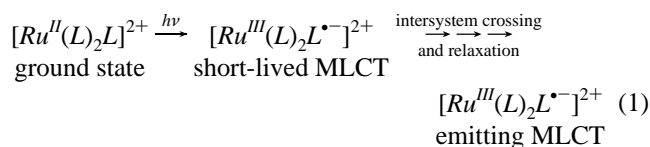


Figure 1. Schematic illustration of $[\text{Ru}(\text{phen})_2\text{dppz}]^{2+}$ and $[\text{Ru}(\text{bpy})_2\text{dppz}]^{2+}$.

of predominantly singlet character, which is converted by intersystem crossing and relaxation to the emitting MLCT species, which is predominantly triplet in character.



The equilibrated emitting MLCT species is formed on an extraordinarily short time scale (<300 fs), see below and elsewhere.³⁰ Optical excitation of $[\text{Ru}(\text{phen})_2\text{dppz}]^{2+}$ and related compounds in the near-ultraviolet affords both MLCT and upper excited states (nominally singlet in character), S_N , but these relax rapidly to the emitting MLCT species.

MLCT luminescence lifetimes are typically in the microsecond range and exhibit a small radiative rate constant ($\sim 10^5 \text{ s}^{-1}$) that reflects the formally-spin-forbidden character of the emission. For $[\text{Ru}(\text{bpy})_3]^{2+}$, the emitting MLCT species has been assigned to a thermal mixture of triplet MLCT states, as well as a weak admixture of singlet MLCT configurations.³¹ An additional, thermally accessible MLCT excited state (the so-called 4th MLCT state) exists for several polypyridyl complexes of Ru(II).³² In general, the decay rate constant of this state is approximately one order of magnitude larger than the decay rate constant observed for the lower manifold of MLCT states. Temperature-dependent lifetime data on a variety of polypyridyl complexes of Ru(II) indicate the additional MLCT state can contribute significantly to excited-state decay at room temperature.³³

The spectroscopy of $[\text{Ru}(\text{phen})_2\text{dppz}]^{2+}$ in nonaqueous solvents (e.g., acetonitrile) is closely analogous to $[\text{Ru}(\text{bpy})_3]^{2+}$.³⁴ Broad, structureless luminescence is observed originating from a long-lived MLCT species (denoted $MLCT'$). For the light-switch complex, however, the addition of proton donors such as acetic acid efficiently quenches $MLCT'$ emission by a bimolecular process at a diffusion-controlled rate.³⁵ This quenching has been attributed to proton transfer from the proton donors (acids) to $MLCT'$, which evidence suggests has a negative charge localized on the dppz ligand.^{3,13,36} $MLCT'$ is believed

to have the following nominal charge distribution, $[\text{Ru}^{\text{III}}(\text{L})_2(\text{dppz}^{\bullet-})]^{2+}$. Thus, the proton transfer has been proposed to occur from the added acid (HA) to the reduced dppz ligand. Alternative mechanisms for quenching $MLCT'$, such as energy transfer and electron transfer, were ruled out on the basis of the fact that the bimolecular quenching was efficient for quenchers that were moderate acids, e.g., acetic acid ($\text{p}K_a = 4.77$), but not good electron and/or energy donors or acceptors.³⁵ Importantly, the ultimate fate of the proposed protonated excited state was not addressed in these previous studies.

In an attempt to evaluate this mechanism we undertook a detailed investigation of the time-resolved emission and absorption spectroscopy of $[\text{Ru}(\text{phen})_2\text{dppz}]^{2+}$. The results of these studies demonstrate that the light-switch mechanism involves a previously unreported exergonic intramolecular charge-transfer process that converts an initially-formed MLCT state (denoted by $MLCT'$) to a novel MLCT state (denoted by $MLCT''$) that emits in the near-infrared and has a small emission yield.

Consistent with the previous proposal, the *proton donating ability of the solvent* is one of the critical properties that allows for the quenching of $MLCT'$. In the present mechanism, however, only partial proton donation is involved, not actual proton transfer. In fact, complete proton transfer is ruled out on energetic and spectroscopic grounds.

Experimental Methods

$[\text{Ru}(\text{phen})_2\text{dppz}]\text{Cl}_2$ was prepared following procedures in the literature² and further purified by reverse-phase liquid chromatography.³⁷ All stock solutions were filtered prior to use. Experiments were carried out in pure water, aqueous buffered solutions (pH 7, 8.5, 10), HCl solutions (pH ≈ 4), and NaOH solutions (pH $\approx 12, 14$) with no significant change in experimental results. Mixtures of acetonitrile and water were prepared by either dilution of an aqueous stock solution with acetonitrile or dilution of an acetonitrile stock solution with water.

Transient-absorption experiments reported employed a laser system based on the design of Squier et al.,^{38,39} and details have been described elsewhere.⁴⁰ In brief, laser pulses (130-fs duration centered near 790 nm with a pulse energy of $\approx 200 \mu\text{J}$) at a 2-kHz repetition rate were generated by a Ti:sapphire-based oscillator and regenerative amplifier. Each laser pulse was split into two parts: pump and probe. The probe portion was used to generate white-light continuum in a spinning quartz disk. The probe light was obtained by wavelength selection of this continuum with use of a circular variable interference filter wheel (Optical Coating Laboratories, Inc.) producing approximately 10 nm of bandwidth. The pump portion of the light was chopped at 1 kHz and optically delayed by a translation stage. Samples were excited by the second harmonic of the amplified laser (≈ 395 nm) with an energy

(29) Kalyanasundaran, K. *Photochemistry of Polypyridine and Porphyrin Complexes*; Academic Press: New York, 1992.

(30) Damrauer, N. H.; Cerullo, G.; Yeh, A.; Bousie, T. R.; Shank, C. V.; McCusker, J. K. *Science* **1997**, *275*, 54–57.

(31) Hager, C. D.; Crosby, G. A. *J. Am. Chem. Soc.* **1975**, *97*, 7031.

(32) Sykora, M.; Kincaid, J. R. *Inorg. Chem.* **1995**, *34*, 5852–5856.

(33) Lumpkin, R. S.; Kober, E. M.; Worl, L. A.; Murtaza, Z.; Meyer, T. J. *J. Phys. Chem.* **1990**, *94*, 239–243.

(34) Nair, R. B.; Cullum, B. M.; Murphy, C. J. *Inorg. Chem.* **1997**, *36*, 962–965.

(35) Turro, C.; Bossman, S. H.; Jenkins, Y.; Barton, J. K.; Turro, N. J. *J. Am. Chem. Soc.* **1995**, *117*, 9026–9032.

(36) Fees, J.; Kaim, W.; Moscherosch, M.; Matheis, W.; Klíma, J.; Krejčík, M.; Zális, S. *Inorg. Chem.* **1993**, *32*, 166–174.

(37) Arkin, M. R. Ph.D. Thesis, California Institute of Technology, 1997.

(38) Squier, J.; Salin, F.; Mourou, G.; Harter, D. *Opt. Lett.* **1991**, *16*, 324–326.

(39) Squier, J.; Korn, G.; Mourou, G.; Vaillancourt, G.; Bouvier, M. *Opt. Lett.* **1993**, *18*, 625–627.

(40) Kliner, D. A. V.; Alfano, J. C.; Barbara, P. F. *J. Chem. Phys.* **1993**, *98*, 5375–5389.

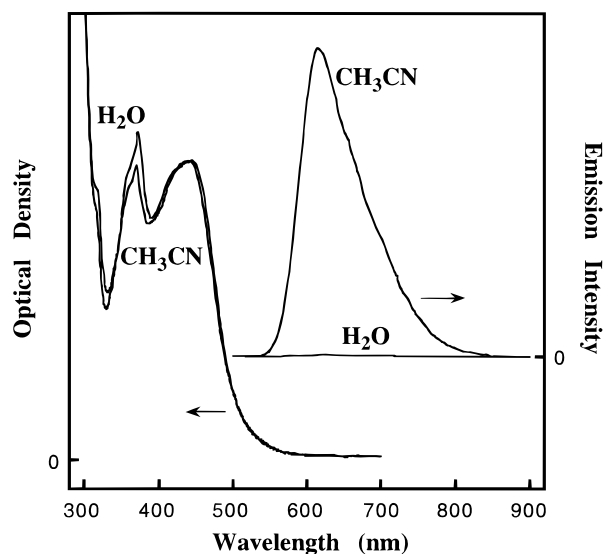


Figure 2. Absorption and emission spectra for $[\text{Ru}(\text{phen})_2\text{dppz}]^{2+}$ in acetonitrile and H_2O .

per pulse of $\approx 8 \mu\text{J}$. The second harmonic was generated in a $100\text{-}\mu\text{m}$ β -BBO crystal, and a half-wave plate was employed to define a magic-angle relationship between the polarization of the pump and probe light. Our instrument response function was $\approx 300\text{-fs}$ full width half maximum (fwhm).

The time-correlated single-photon counting apparatus utilizes a home-built cavity-dumped femtosecond mode-locked Ti:sapphire laser centered near 830 nm . Samples were excited with frequency doubled light (415 nm) at a variable repetition rate (e.g., 1 MHz). Emission was collected at 90° through a computer-controlled circular variable interference filter wheel (Optical Coating Laboratories, Inc.) and/or an adjustable polarizer. Emission was detected with a microchannel plate photomultiplier tube (Hamamatsu R3809U-01) or an avalanche photodiode (EG&G Canada SPCM-203-PQ) at count rates of $\approx 1 \text{ kHz}$. Decay curves were accumulated in a multichannel analyzer (Tracor Northern TN-7200). All emission decay data were transferred to a personal computer and fit to a sum of exponentials convolved with the appropriate instrument response function employing a nonlinear least-squares weighted-residuals routine. The instrument response function was measured by using a dilute suspension of non-dairy creamer to scatter laser pulses into the direction of the detector. The microchannel plate photomultiplier tube produced an instrument response function with fwhm $\approx 30 \text{ ps}$. The avalanche photodiode detector produced an instrument response function with fwhm $\approx 200 \text{ ps}$. Time-gated spectra were collected with a single channel analyzer (EG&G ORTEC 550A) and corrected for detector response. All measurements were performed at ambient temperature ($21 \pm 2 \text{ }^\circ\text{C}$).

Results

Luminescence Measurements. The steady-state luminescence and absorption spectra of $[\text{Ru}(\text{phen})_2\text{dppz}]^{2+}$ in acetonitrile and water are shown in Figure 2. The similarity of the absorption spectra in the two solvents strongly suggests that the electronic character and energies of the Franck–Condon singlet excited MLCT ($\lambda_{\text{max}} \approx 440 \text{ nm}$) and π,π^* ligand centered excited states ($\lambda_{\text{max}} \approx 380 \text{ nm}$) are not significantly solvent dependent. In contrast, the steady-state emission is dramatically different in the two solvents. Moderately strong emission from a MLCT species is easily observed in acetonitrile, while in water no significant emission is apparent with use of a conventional fluorimeter. Acetonitrile/water solvent mixtures are intermediate in behavior, showing significantly less MLCT emission than pure acetonitrile. It has been suspected that the lack of emission in aqueous environments is due to rapid, water-induced quenching of the MLCT state, but kinetic observation of the quenching has not been previously published.

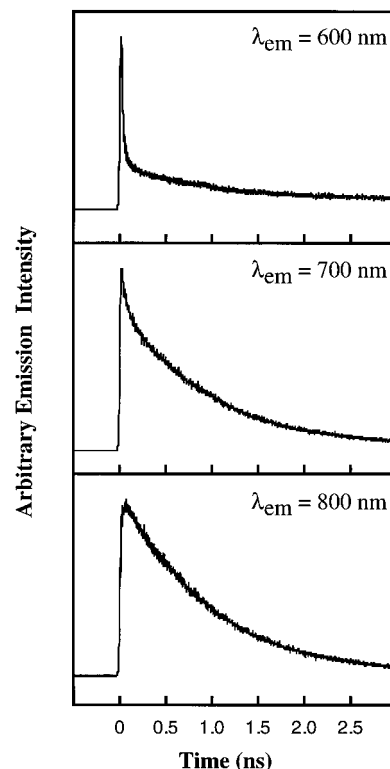


Figure 3. Representative decays for $[\text{Ru}(\text{phen})_2\text{dppz}]^{2+}$ in an acetonitrile/water mixed solvent system (1:2 (v/v)). The decays are well fit by a three-exponential decay function with $\tau_1 = 10 \text{ ps}$, $\tau_2 = 0.95 \text{ ns}$, $\tau_3 \gg 10 \text{ ns}$. At 600 nm , the relative percent amplitudes for each component are $A(\tau_1) = 93$, $A(\tau_2) = 5$, and $A(\tau_3) < 2$. At 700 nm , the relative percent amplitudes for each component are 77 , 23 , and < 1 . At 800 nm , the relative percent amplitudes for each component are 51 , 49 , and < 1 .

The time-resolved emission of $[\text{Ru}(\text{phen})_2\text{dppz}]^{2+}$ in a 1:2 by volume solvent mixture of acetonitrile/water at selected emission wavelengths is shown in Figure 3. The standard technique for measuring ultrafast time-resolved emission dynamics is fluorescence upconversion. This technique is not sufficiently sensitive to measure the emission dynamics of species like MLCT states that have extremely small radiative rates ($k_{\text{rad}} \approx 10^5 \text{ s}^{-1}$). Instead, we employ the more sensitive technique, time-correlated single photon counting (TCSPC), which possesses an instrument response function with a fwhm $\approx 30 \text{ ps}$ (in our laboratory) and can resolve dynamics with decay times as small as 10 ps . The fluorescence dynamics evolve on two time scales, i.e., a very fast $10 \pm 4 \text{ ps}$ component which is barely resolvable with our apparatus, and an intermediate $950 \pm 70 \text{ ps}$ component. Figure 4 shows time-resolved emission spectra that were determined by spectral reconstruction from multiexponential fits to the time-resolved data of the type in Figure 3. At early times ($0\text{--}5 \text{ ps}$), the emission spectrum is peaked near 600 nm consistent with the MLCT emission spectra typically observed for this class of compounds. For reference we denote the species with the 600-nm emission as MLCT' . The MLCT' band decays (τ_{obs}) in $10 \pm 4 \text{ ps}$, apparently forming an intermediate species, MLCT'' . MLCT'' has a much less intense spectrum, which is peaked at $\sim 750 \text{ nm}$ and decays (τ_{obs}) in $950 \pm 70 \text{ ps}$. The chemical nature of the $\text{MLCT}' \rightarrow \text{MLCT}''$ interconversion is addressed in the Discussion section.

Table 1 summarizes the various photodynamic quantities for MLCT' and MLCT'' estimated by analyzing the transient-emission data of $[\text{Ru}(\text{phen})_2\text{dppz}]^{2+}$ in pure acetonitrile, pure water, and 1:2-acetonitrile/water. On the basis of the wavelength maximum and band shape we assign MLCT' in all

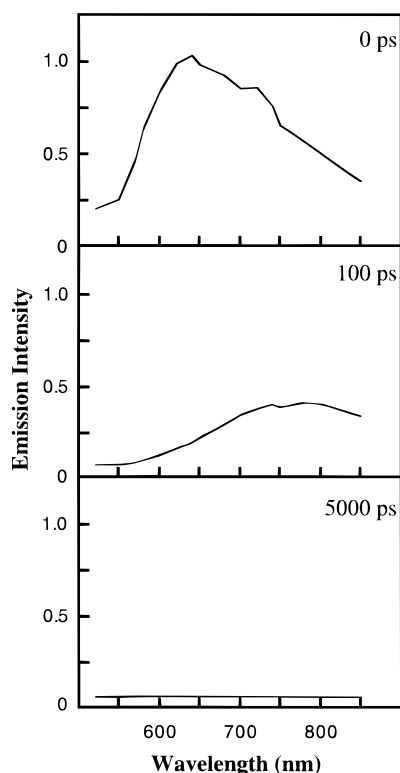


Figure 4. Time-resolved emission spectra for $[\text{Ru}(\text{phen})_2\text{dppz}]^{2+}$ in an acetonitrile/water mixed solvent system (1:2 (v/v)). Spectra are reconstructed from fits to the decays collected at 15 wavelengths and corrected for detector sensitivity. Each transient was fit with a three-exponential decay function convolved with our instrument response function. At each wavelength, τ_1 was fixed at 0.01 ns, τ_3 was fixed at 100 ns, and $\tau_2 \approx 0.95$ ns, and all three amplitudes were free-floating parameters in the fit.

Table 1. Quantum Yields and Lifetimes for $[\text{Ru}(\text{phen})_2\text{dppz}]^{2+}$ in H_2O , Acetonitrile, and an Acetonitrile/ H_2O Mixed Solvent System^a

solvent	Φ_{lum}	τ_{obs}	$k_{\text{rad}} (\text{s}^{-1})$
CH_3CN	$MLCT^b$ 0.033	660 ns ^d	$\approx 10^5$
H_2O	$MLCT^c$ 3×10^{-7}	3 ps	$\approx 10^5$
	$MLCT''^c$ 2.5×10^{-6}	250 ps	$\approx 10^4$
1:2 acetonitrile/water	$MLCT^c$ 1.0×10^{-6}	10 ps	$\approx 10^5$
	$MLCT''^c$ 9.5×10^{-6}	950 ps	$\approx 10^4$

^a See text for procedures that were used to estimate the various quantities. ^b Quantum yield for $[\text{Ru}(\text{phen})_2\text{dppz}]^{2+}$ in CH_3CN measured by Nair *et al.*³⁴ ^c The quantum yields for $MLCT'$ and $MLCT''$ were estimated, using the relationship $\Phi_{\text{lum}} = k_{\text{rad}} \tau_{\text{obs}}$. On the basis of error estimates for k_{rad} , our error estimate for Φ_{lum} is $\sim 50\%$. ^d Solution prepared in air and purged with N_2 and well fit to a single-exponential decay. See text for error estimates.

solvents to the typical $MLCT$ state for polypyridyl–ruthenium complexes. Indeed, the initial (early-time) intensity of the $MLCT'$ spectrum in 1:2 acetonitrile/water is within experimental error (a factor of ≤ 2) of the corresponding emission measured by the same procedure from $[\text{Ru}(\text{phen})_2\text{dppz}]^{2+}$ in pure acetonitrile at the same concentration. By analogy to the pure acetonitrile results, this is evidence that the radiative rate, k_{rad} , of $MLCT'$ in 1:2 acetonitrile/water is approximately the same as k_{rad} for pure acetonitrile (very recently k_{rad} for $[\text{Ru}(\text{phen})_2\text{dppz}]^{2+}$ has been reported to vary little as a function of solvent polarity³⁴). Kinetic simulations⁴¹ of the TCSPC measurements assuming efficient $MLCT' \rightarrow MLCT''$ interconversion indicate that the excited state exhibiting 800-nm emission ($MLCT''$) possesses a radiative rate approximately one order of magnitude smaller than the excited state responsible for the 600-nm

emission ($MLCT'$). Finally, we have estimated the quantum yields for $MLCT'$ and $MLCT''$ by using the measured lifetimes and the estimated radiative rates, using the relationship $\Phi_{\text{lum}} = k_{\text{rad}} \tau_{\text{obs}}$. Direct measurements of the quantum yields were not possible in 1:2 acetonitrile/water and in water due to the small emission yield, the presence of weak fluorescent impurities, and the wavelength region of the $MLCT''$ emission which is beyond the sensitivity range for available detectors that could be dependably calibrated.

An unfortunate complication in Figures 3 and 4 is the presence of a weak long-lived (> 10 ns) impurity with a spectrum that resembles emission from polypyridyl–ruthenium complexes. The relative intensities of the early-time and late-time emission suggests the impurity is present at $< 1\%$ molar concentration. The impurity emission is not easily apparent in the data in Figure 4, but it can be observed if the > 5000 -ps spectrum is significantly enlarged. The impurity is more apparent in the raw transient data, especially in the region of the $MLCT'$ emission. The $MLCT'$ emission is artificially weak due to the limited time resolution of the apparatus and the short lifetime of the $MLCT'$ emission.

The 10-ps $MLCT' \rightarrow MLCT''$ interconversion implies that there should be a delayed appearance of the $MLCT''$ population, and consequently, a delayed appearance (or rise time) of the $MLCT''$ emission (e.g., 800-nm transient). In fact, no delayed appearance has been observed, but its absence may be due to practical complications. First, the time resolution of the TCSPC apparatus is not sufficient to detect the appearance kinetics of $MLCT''$. Second, the red portion of the $MLCT'$ emission is broad and substantially overlaps the $MLCT''$ band. Third, the oscillator strength of the $MLCT''$ band is weaker than that for the $MLCT'$ band.

Figure 5 shows emission transients in pure water. The $MLCT'$ band decays so rapidly in this solvent that the dynamics at 600 nm follow the instrument response function (30-ps fwhm) and the $MLCT' \rightarrow MLCT''$ interconversion is too rapid to resolve with TCSPC (ultrafast pump/probe transient-absorption measurements, which are described below, estimate the time scale to be 3 ± 1 ps). Due to the short $MLCT'$ lifetime (as compared to the width of the instrument response function), the peak intensity of the observed emission is significantly diminished relative to pure acetonitrile and 1:2 acetonitrile/water. As a result, the extremely weak long-lived emission attributed to an impurity is easily observed in the 600-nm decay. At 800 nm the emission dynamics primarily reflect the decay of $MLCT''$, yielding a lifetime of 250 ± 15 ps.

Figure 6 shows time-resolved emission transients from emission at wavelengths longer than 715 nm on a 5-ns time window. These data, which are reasonably well fit by a single exponential decay reflect the decay of $MLCT''$ in H_2O and D_2O , yielding excited-state lifetimes of 250 ± 15 and 580 ± 40 ps, respectively (on this time scale the interconversion process is too fast to resolve, and the impurity emission is not a significant factor ($< 1\%$) at these wavelengths). Experiments in a wide range of buffered and unbuffered solutions reveal that the observed kinetics do not demonstrate an appreciable dependence on pH across greater than 8 pH units. It will be shown below that the decay of $MLCT''$ should be assigned to the recovery of the ground state, $[\text{Ru}(\text{phen})_2\text{dppz}]^{2+}$.

(41) Excited-state equilibria were simulated by using a simplified first-order reaction scheme connecting four species. Time-dependent emission intensities were predicted from the time-dependent concentrations of the four species expressed in terms of the four rate constants defined in the simplified first-order scheme. See, for example: Moore, J. W.; Pearson, R. G. *Kinetics and Mechanism*, 3rd ed.; John Wiley & Sons: New York, 1981; p 296.

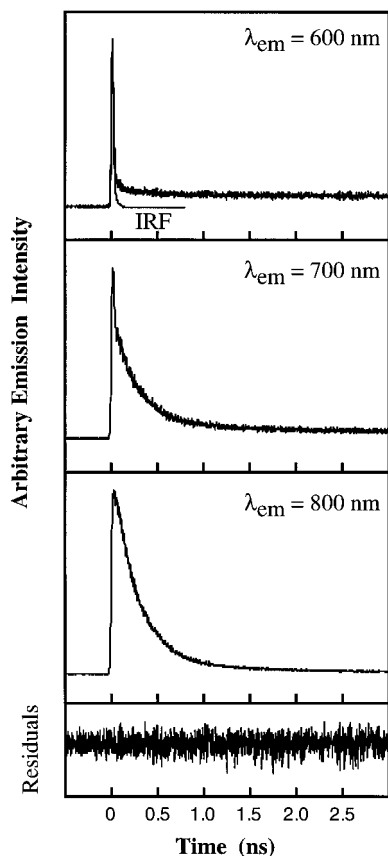


Figure 5. Representative decays for $[\text{Ru}(\text{phen})_2\text{dppz}]^{2+}$ in pure water. The lifetime components of the fits, with relative percent amplitudes in parentheses, are consistent with the mixed solvent data in Figure 4. At 600 nm the observed emission decay is well fit with a three-exponential decay function with $\tau_1(98)$ fixed at 3 ps, $\tau_2(<1) \approx 0.25$ ns, and $\tau_3(1)$ fixed at 100 ns. Emission decays collected at 700 nm can also be well fit with a three-exponential decay function with $\tau_1(88)$ fixed at 3 ps, $\tau_2(11) \approx 0.25$ ns, and $\tau_3(<1)$ fixed at 100 ns. The 800-nm data are well fit with a biexponential decay function with $\tau_1(95) \approx 0.25$ ns and $\tau_2(5) \approx 8$ ns. Weighted residuals for the 800-nm data are shown in the bottom panel.

Time-gated emission spectra for $[\text{Ru}(\text{phen})_2\text{dppz}]^{2+}$ in various environments are shown in Figure 7. The emission spectra in acetonitrile at various times during the excited-state lifetime are indistinguishable from the time-integrated emission spectrum. As described earlier, this emission has a similar band shape and lifetime to the usual MLCT bands exhibited by compounds such as $[\text{Ru}(\text{bpy})_3]^{2+}$. It is interesting that the relaxed emission spectrum of 1:1 acetonitrile/water is intermediate between that for acetonitrile and pure water. It is likely that the spectrum for 1:1 acetonitrile/water represents emission from MLCT' in this environment. Thus, the MLCT' spectrum apparently is extremely solvent dependent. Alternatively, the emission spectrum in 50% H_2O may be a superposition of MLCT' and MLCT'' emission, both present in equilibrium in the relaxed excited state.

We have also examined the time-gated spectra of the relaxed emission spectra in pure D_2O solvent (data not shown). The MLCT'' spectra in pure H_2O and D_2O are identical within experimental error. As mentioned above, however, the lifetimes of the relaxed excited state in H_2O vs D_2O differ by more than a factor of 2.

Transient-Absorption Spectroscopy. The faster time resolution of transient-absorption spectroscopy, coupled to its ability to probe multiple ground-state and excited-state absorption bands, makes this technique a powerful tool for characterizing

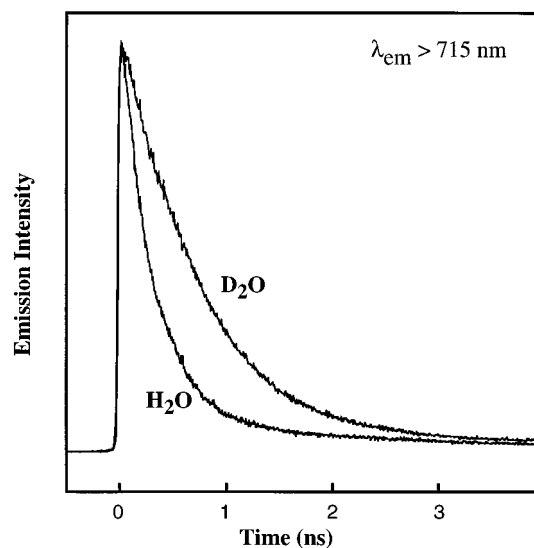


Figure 6. Normalized TCSPC emission decay dynamics for $[\text{Ru}(\text{phen})_2\text{dppz}]^{2+}$ in H_2O and D_2O with 400-nm excitation and collected at magic-angle polarization through a 715-nm long-pass filter. The decays are well fit to a single exponential decay, $\tau_{\text{H}_2\text{O}} \approx 0.25$ ns and $\tau_{\text{D}_2\text{O}} \approx 0.58$ ns, demonstrating a solvent isotope effect on the luminescence lifetime of ≈ 2.3 .

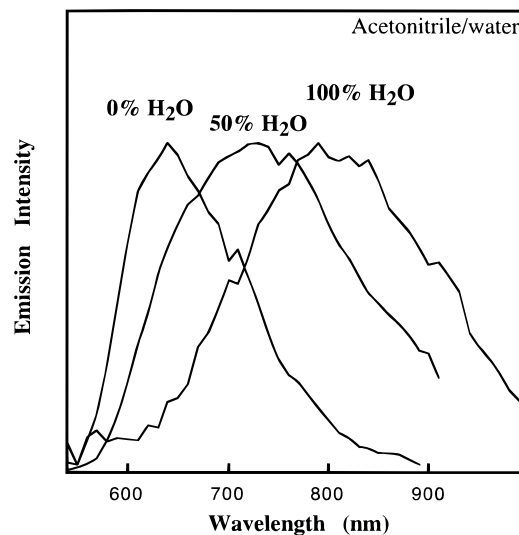


Figure 7. Time-gated emission spectra for $[\text{Ru}(\text{phen})_2\text{dppz}]^{2+}$ in select acetonitrile/water mixed solvent systems collected by TCSPC with a single-channel analyzer. The emission time window was centered 200 ps after photoexcitation with a width of ≈ 200 ps. Spectra are corrected for spectrometer sensitivity.

the photodynamics of $[\text{Ru}(\text{phen})_2\text{dppz}]^{2+}$. The transient-absorption spectroscopy of this complex in H_2O evolves on two different time scales, i.e. 3 ± 1 and 250 ± 10 ps. It will be demonstrated shortly that the faster of these two time scales corresponds to the formation of the relaxed excited state (MLCT') of the complex. The slower dynamics, on the other hand, are associated with ground-state recovery from the MLCT'' excited state.

The early-time transient-absorption kinetics in H_2O are shown in Figure 8. The 440-nm transient probes the ground-state absorption (see Figure 2). The negative signal (bleach) corresponds to depletion of the ground state induced by the excitation pulse at zero time. The absence of significant bleach recovery during the first 15 ps indicates that very little ground-state recovery occurs during this time period.

Transients at longer wavelengths probe absorption bands of the electronically excited complex. By analogy to previous

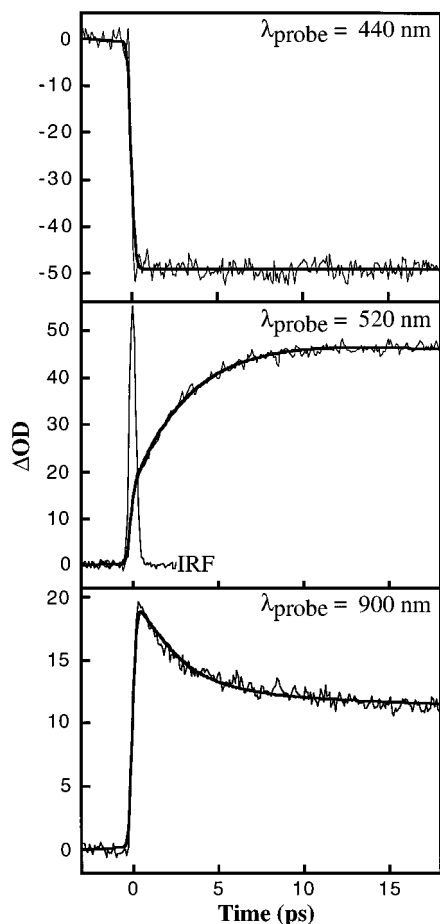


Figure 8. Pump/probe transient-absorption dynamics for $[\text{Ru}(\text{phen})_2\text{dppz}]^{2+}$ in pure water on a 20-ps time window employing 440, 520, and 900-nm probe lights. Data indicate the early-time (time = 0) excited-state species possesses an absorption spectrum that is red-shifted relative to the equilibrated excited-state species demonstrating the 250-ps decay. Lifetime components, with percent amplitude in parentheses, for the fits shown are as follows: 440-nm probe, $\tau_1(100)$ fixed at 1000 ps; 520-nm probe, $\tau_1(-66) = 3 \pm 1$ ps and $\tau_2(100)$ fixed at 250 ps; 900-nm probe, $\tau_1(41) = 3 \pm 1$ ps and $\tau_2(59)$ fixed at 250 ps.

experiments on related complexes, the long wavelength absorptions of the excited state correspond to π, π^* excitations of ligands with excess charge, i.e. analogous to a radical anion.^{2,14,30} This in turn corresponds to the MLCT character of the excited state.

The absorption kinetics at 900 and 520 nm are consistent with the interconversion of two MLCT excited states. The absorption band of the initial form is considerably red shifted, while the delayed form apparently has an absorption that peaks in the visible. The kinetics at the two wavelengths are well fit by a biexponential function with a 3 ± 1 ps component contributing the resolved dynamics. The dynamics in Figure 8 are apparently due to the $MLCT' \rightarrow MLCT''$ interconversion. These dynamics are not observed in DNA environments (see below). It is unlikely that the observed 3-ps process should be assigned to intersystem crossing of S_N and early relaxation of the initially-formed MLCT. By analogy to related complexes, these dynamics should be much more rapid than 3 ps.³⁰ The absence of the 3-ps dynamics in the presence of DNA is further evidence against an intersystem crossing assignment for the 3-ps component since intersystem crossing does occur for $[\text{Ru}(\text{phen})_2\text{dppz}]^{2+}$ in DNA.

It is noteworthy that the $MLCT' \rightarrow MLCT''$ interconversion apparently occurs without any competitive repopulation of the ground state. Thus, this implies that the major kinetic process

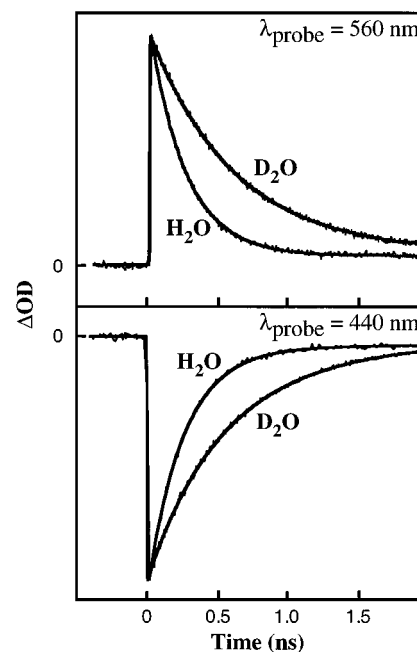


Figure 9. Pump/probe transient-absorption measurements employing a 400-nm pump light and 560- or 440-nm probe lights monitoring the transient excited-state absorption and MLCT bleach-recovery dynamics for photoexcited $[\text{Ru}(\text{phen})_2\text{dppz}]^{2+}$ in H_2O and D_2O . Lifetime components, with percent amplitude in parentheses, for the fits shown are as follows: H_2O data at 440 nm, $\tau_1(-96) = 250 \pm 8$ ps and $\tau_2(-4)$ fixed at 100 000 ps; H_2O data at 560 nm, $\tau_1(98) = 250 \pm 15$ ps and $\tau_2(2)$ fixed at 100 000 ps; D_2O data at 440 nm, $\tau_1(-97) = 560 \pm 15$ ps and $\tau_2(-3)$ fixed at 100 000 ps; D_2O data at 560 nm, $\tau_1(98) = 580 \pm 20$ ps and $\tau_2(2)$ fixed at 100 000 ps.

for the excited-state relaxation leads to formation of $MLCT'$ from the Franck-Condon excited state (within 300 fs) with a quantum yield of formation of unity. In water, this is followed by $MLCT' \rightarrow MLCT''$ interconversion on the 3-ps time scale with a quantum yield near unity.

The decay mechanism of $MLCT''$ is addressed by an examination of the longer time scale transient absorption kinetics, as shown in Figure 9. The excited-state absorption of $MLCT''$ at 520 nm decays with time constants that closely correspond to the emission decays of these species, i.e., $\tau_{\text{H}_2\text{O}} = 250 \pm 8$ ps and $\tau_{\text{D}_2\text{O}} = 560 \pm 20$ ps. Correspondingly, the ground-state absorption recovery kinetics exactly parallels the excited-state absorption decay within experimental error. This set of observations allows us to assign the 250 ± 8 ps lifetime in water to the radiationless decay process (nominally intersystem crossing) that connects $MLCT''$ to the ground state without any apparent intermediate.

Transient-Absorption Dynamics in DNA Environments.

Figure 10 compares the transient-absorption kinetics of $[\text{Ru}(\text{phen})_2\text{dppz}]^{2+}$ in aqueous solution in the absence and presence of DNA. As mentioned elsewhere, in DNA environments partial intercalation of the complex results in dynamics similar to those in nonaqueous environments. In particular, the emission quantum yield is substantial and the excited-state lifetime is on the hundreds of nanosecond time scale.^{6,7} The nanosecond time scale absorption transients are highly consistent with this picture. The initial bleach of the ground state does not show significant recovery and the excited-state absorption (due to $MLCT'$ not $MLCT''$) appears unresolvably fast. Shorter time scale measurements reveal no dynamics, indicating $MLCT' \rightarrow MLCT''$ interconversion is suppressed and no significant ground-state recovery occurs on the picosecond time scale.

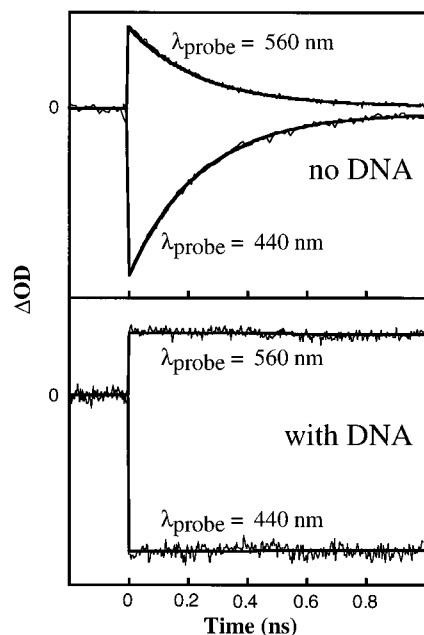


Figure 10. Pump/probe transient-absorption dynamics for $[\text{Ru}(\text{phen})_2\text{dppz}]^{2+}$ in aqueous solution in the absence and presence of DNA. In both panels, MLCT bleach-recovery dynamics are probed with 440-nm light and photoinduced transient-increased absorption was probed with 560-nm light. Lifetime components, with percent amplitude in parentheses, for the fits shown are as follows: no DNA data at 440 nm, $\tau_1(-96) = 250 \pm 8$ ps and $\tau_2(-4)$ fixed at 100 000 ps; no DNA data at 560 nm, $\tau_1(98) = 250 \pm 15$ ps and $\tau_2(2)$ fixed at 100 000 ps; with DNA data at 440 nm, $\tau_1(-100)$ fixed at 100 000 ps; with DNA data at 560 nm, $\tau_1(100)$ fixed at 100 000 ps.

Discussion

The various transient absorption and transient emission data for $[\text{Ru}(\text{phen})_2\text{dppz}]^{2+}$ are highly consistent with the kinetic model in Figure 11. According to this model, the weak emission of the complex in water and in acetonitrile/water environments is due to rapid conversion of the $MLCT'$ state to a different emitting excited state $MLCT''$, which itself has a rapid radiationless decay pathway. The $MLCT'$ state is assigned to the usual type of MLCT state exhibiting 600-nm emission. $MLCT'$ is rapidly converted to $MLCT''$, induced by an interaction with water.

Thus, the light-switch mechanism in water can be attributed to an excited-state interconversion of the initially formed $MLCT'$ to a different emitting form $MLCT''$. $MLCT'$ is analogous to the MLCT-emitting form of $[\text{Ru}(\text{phen})_2\text{dppz}]^{2+}$ in pure acetonitrile (and presumably DNA). We have estimated the quantum yield of the $MLCT'$ emission in water by using the time-resolved emission spectra, which are less susceptible to impurity emissions, see Table 1. The extraordinarily small quantum yield of the $MLCT'$ emission can be attributed to the rapid ($\tau \approx 3$ ps) $MLCT' \rightarrow MLCT''$ interconversion. On the other hand, the $MLCT''$ state is itself emissive. The low quantum yield of this state is largely a consequence of its rapid radiationless decay ($\tau \approx 250$ ps). In summary, the light-switch mechanism involves two steps, namely $MLCT' \rightarrow MLCT''$ interconversion and $MLCT''$ radiationless decay.

To unravel the chemical nature of the light-switch mechanism it is necessary to explore the electronic structures of the $MLCT'$ and $MLCT''$ intermediates. Additionally, it is necessary to assign the $MLCT' \rightarrow MLCT''$ interconversion process and the $MLCT''$ ground-state decay to specific dynamical processes. In particular, it is important to determine whether either dynamical process is indeed proton transfer with the solvent.

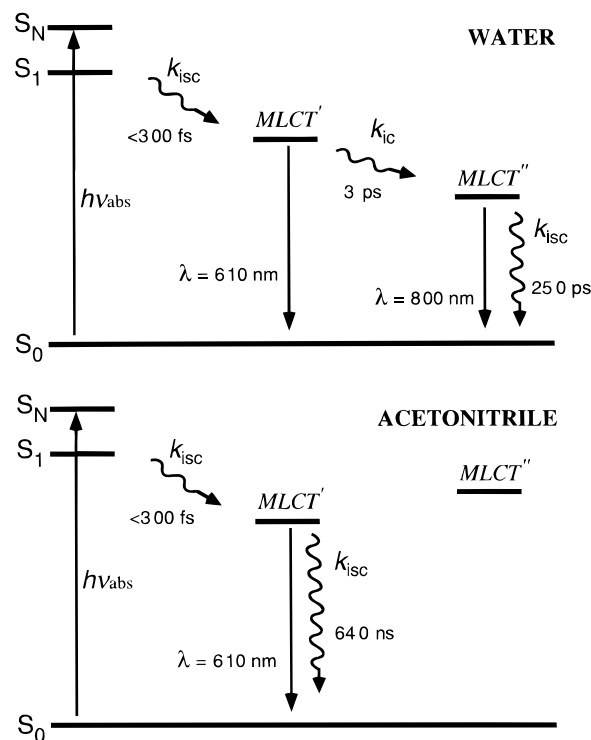
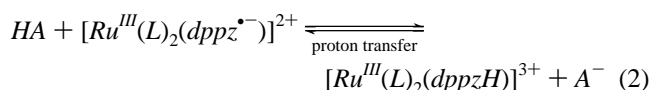


Figure 11. Outline of the model describing the environment-dependent photophysics of $[\text{Ru}(\text{phen})_2\text{dppz}]^{2+}$. $MLCT'$ and $MLCT''$ denote distinct MLCT excited states distinguished by the distribution of charge on the metal–ligand framework.

The Structure of $MLCT''$. One hypothetical structure for $MLCT''$ which would be consistent with a proton-transfer mechanism is simply a protonated MLCT state, $[\text{Ru}(\text{phen})_2(\text{dppzH})]^{3+}$. This could arise in principle for *adiabatic excited state proton transfer*,



where HA is the acid, either H_3O^+ or H_2O itself in aqueous solutions. This hypothetical process (eq 2) would seem to be consistent with the observation that moderate acids dynamically quench the MLCT emission of photoexcited $[\text{Ru}(\text{phen})_2\text{dppz}]^{2+}$ in acetonitrile, which has been taken as evidence for bimolecular, diffusion-controlled quenching where the specific structure or electronic state of the product were not specified.³⁵

There are kinetic and thermodynamic arguments against this mechanism. The possibility that H_3O^+ is involved in the formation of $MLCT''$, or for that matter that H_2O is involved in any aspect of the dynamics, can be ruled out since the transient spectroscopy of $[\text{Ru}(\text{phen})_2\text{dppz}]^{2+}$ is not a function of pH over a large range (>8 pH units). The possibility that H_2O itself might directly protonate the $MLCT'$ state can be addressed on thermodynamic grounds. H_2O is a weak acid ($\text{p}K_a \approx 15$). Since the $MLCT' \rightarrow MLCT''$ interconversion is rapid at room temperature, the actual driving force for the reaction must be close to zero if not substantially exergonic. Furthermore, since typical excited-state protonation reactions are reversible, the observation that $MLCT''$ is a clear dominant species after the reaction is complete implies that the proton-transfer reaction would have to be exergonic by at least $20 \text{ kJ}\cdot\text{mol}^{-1}$ to be consistent with experiment.

To exhibit exergonic proton transfer from water, $MLCT'$ would have to be an extremely strong base. In particular, the $\text{p}K_a$ of the conjugate acid of $MLCT'$ would have to be greater

than 16. This, however, is highly unlikely. MLCT states of analogous compounds exhibit pK_a values in the range of 1.5–4.4.⁴² An example of a compound in this group is [Ru(bpy)₂bpz]²⁺, where bpz is 2,2'-bipyrazine. The relatively weak basicity of MLCT states has been attributed to the presence of the highly positively charged (3+) metal center near the basic ligand.

Evidence supporting the importance of the charge on the metal center is found in the previous observation that the monoreduced complexes are stronger bases than the MLCT excited states. The following empirical relationship has been observed to hold for a broad range of complexes,

$$pK_a(\text{reduced ground state}) - pK_a(\text{MLCT}) = 4.8 \quad (3)$$

where pK_a refers to the conjugate acid of each species.^{42,43} Using this relationship and the known pK_a of the conjugate acid of the reduced form of [Ru(bpy)₂dppz]²⁺ (pK_a ≈ 10),⁴⁴ the pK_a of the conjugate acid of the MLCT state of [Ru(bpy)₂dppz]²⁺ should be approximately 5. By analogy we assume that the conjugate acid of MLCT' for [Ru(phen)₂dppz]²⁺ is also on the order of 5. On the basis of these arguments it can be concluded that the equilibrium in eq 2 must substantially favor the left-hand side with H₂O as the acid. The 600-nm decay observed in water (Figure 5) is inconsistent with this interpretation. Thus, adiabatic excited-state proton transfer can be ruled out, and it is highly unlikely that MLCT'' is a protonated MLCT species.

As an alternative explanation to proton transfer, we propose that MLCT' and MLCT'' represent two different excited state configurations that differ by their distribution of negative charge on the ligands, and associated small geometric changes. Furthermore, it is proposed that MLCT'' as compared to MLCT' has a greater charge density on the phenazine nitrogens. Due to this excess charge density on nitrogen, MLCT'' would be expected to be stabilized relative to MLCT' in polar and hydrogen-bonding solvents, especially in strong proton-donating solvents. Thus, as shown in Figure 11, the absence of the MLCT'' emission in acetonitrile could simply be due to a much higher energy of MLCT'' in this solvent. This proposal is also consistent with the apparent blue shift of the MLCT'' emission in 50% water versus pure water (Figure 7).

Little information is available about the nature of the MLCT''/solvent interactions that are responsible for the observed solvent effects. On the basis of the general sensitivity of the photo-physics of [Ru(phen)₂dppz]²⁺ to proton-donating solvents³⁴ (and added quenchers³⁵) it is likely that in proton-donating solvents, especially water, one or even two hydrogen bonds exist between water and MLCT''. This type of specific and discrete solute/solvent structure could account for the dramatic solvent dependence of the spectroscopy and dynamics of this complex. It should be emphasized that while the basicity of these MLCT states is not sufficient to deprotonate water, they are sufficiently basic to be moderate proton acceptors. Thus, hydrogen-bond formation should be considered as one of the possible factors that promotes the MLCT' → MLCT'' interconversion.

It should also be emphasized that there is spectroscopic evidence that the MLCT' and MLCT'' species are not merely differently solvated forms of the same emitting species. The difference in radiative rates is evidence that they are comprised of predominantly different electronic configurations. Thus, the term *intramolecular charge transfer* is consistent with this result.

Interestingly, MLCT'' may be related to the so-called, 4th MLCT state, which is a high-energy MLCT state with extraordinarily rapid radiationless decay rates that is apparently thermally accessed in the photophysics of certain polypyridyl Ru complexes.^{32,33}

Dynamical Processes. We have not undertaken a detailed kinetic investigation of the MLCT' → MLCT'' interconversion kinetics as a function of temperature and solvent, which would be necessary to determine what process or processes control the observed rate. On the basis of the extensive literature on excited-state intramolecular charge transfer in organic compounds, it is known that a number of processes can control the rate, depending on the chemical system and its environment.⁴⁵ These processes include the following: (i) thermal activation in examples that are barrier controlled, (ii) dynamics of the solvent in strongly adiabatic reactions, (iii) large amplitude intramolecular motions in certain examples, and (iv) ultrafast electronic radiationless decay in examples where two strongly coupled states exist in a "nested" topography. Few data are available to evaluate whether these processes are important for [Ru(phen)₂dppz]²⁺.

Nevertheless, the time scale of the apparent MLCT' → MLCT'' interconversion in water rules out nonspecific solvation dynamics as the rate-limiting process, since 3 ps is considerably slower than the time scale for solvation dynamics in water. On the other hand, 3 ps might be close to the time scale for hydrogen bond formation. In principle, the rate-limiting process for forming MLCT'' could be as follows:



where the dotted bond signifies a hydrogen bond.

This specific proposed interpretation for the 3-ps dynamic component would require that the [Ru(phen)₂dppz]²⁺ ground state is not hydrogen bonded at equilibrium since MLCT' is formed within 300 fs after excitation of the equilibrated ground state. The absence of a hydrogen bond in the ground state is consistent with the extremely weak basicity of these ground states due to the positively-charged metal center.

The rapid radiationless decay of MLCT'' is an additional critical element of the overall light-switch mechanism. The extraordinarily rapid radiationless decay rate for MLCT'' may be associated with hydrogen bonding with H₂O. As described above, hydrogen bonding should be much weaker in the ground state than in MLCT''. Differential hydrogen bonding between ground and excited states has been associated with enhanced radiationless decay for organic compounds⁴⁵ and may play a role for [Ru(phen)₂dppz]²⁺. The significant solvent isotope effect on the rate of radiationless decay from MLCT'' may be evidence that solute/solvent hydrogen bonds with the phenazine nitrogens are indeed accepting modes for the radiationless decay. On the other hand, a H₂O/D₂O isotope effect of comparable magnitude has been observed for the MLCT state of [Ru(bpy)₃]²⁺, which lacks nonbridging nitrogens on the metal/ligand framework.⁴⁶ It has been speculated that the isotope effect for [Ru(bpy)₃]²⁺ is due to H₂O accepting modes involving hydrogenic vibrations of water. Thus, the isotope effect observed for [Ru(phen)₂dppz]²⁺ is not definitive proof of specific

(42) Sun, H.; Hoffman, M. Z. *J. Phys. Chem.* **1993**, *97*, 5014–5018.

(43) Sun, H.; Hoffman, M. Z.; Mulazzani, Q. G. *Res. Chem. Intermed.* **1994**, *20*, 735–754.

(44) Mulazzani, Q. G.; D'Angelantonio, M.; Venturi, M.; Boillot, M.-L.; Chambron, J.-C.; Amouyal, E. *New J. Chem.* **1989**, *13*, 441–447.

(45) Barbara, P. F.; Walsh, P. K.; Brus, L. E. *J. Phys. Chem.* **1989**, *93*, 29–34.

(46) Van Houten, J.; Watts, R. J. *J. Am. Chem. Soc.* **1975**, *97*, 3843–3844.

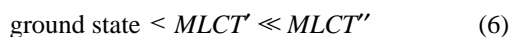
(phenazine-localized) hydrogen bonding or proton transfer involvement in the radiationless decay of $MLCT''$.

A different explanation for the rapid radiationless decay rate of $MLCT''$ may be related to the energy gap law. In particular, the radiationless decay rates of certain MLCT excited states have been demonstrated to decrease exponentially as the energy gap between the ground and excited state is increased, as predicted by the energy gap law.⁴⁷ Thus, for $[Ru(phen)_2dppz]^{2+}$, the lowering of the MLCT excited-state energy by hydrogen-bonding solvation may indirectly accelerate the nonradiative decay rate due to the energy gap law.

An interesting closely-related example of a dramatic solvent effect on emission yields is found in the photophysics of $[fac-(dppz)Re(CO)_3(4-MePh)]^+$ (where 4-MePy = 4-methylpyridine).¹² In this case, the increased oxidation potential of Re(I) serves to shift the corresponding MLCT excited states of this complex to higher energy relative to $[Ru(phen)_2dppz]^{2+}$. As a result, the photophysics of the Re(dppz) system is dominated by the emissive, low-lying, dppz-based intraligand triplet state(s). Analogous to the light-switch behavior of $[Ru(phen)_2dppz]^{2+}$, the Re(dppz) system is *nonluminescent* in water, but moderately luminescent when the complex is bound to DNA or in homogeneous nonaqueous solution.¹² The nonluminescent behavior of Re(dppz) in water is attributed to a low-lying short-lived MLCT state, as in the case of $[Ru(phen)_2dppz]^{2+}$. There is, however, no evidence that the dppz-based intraligand triplet state is a factor in the photophysics of $[Ru(phen)_2dppz]^{2+}$.

Unified Picture of the Photophysics of $[Ru(phen)_2dppz]^{2+}$ in Different Environments. The extremely varied and complex spectroscopy of $[Ru(phen)_2dppz]^{2+}$ is difficult to model with a single, unified mechanism. Nevertheless, we have been able to construct a qualitative photophysical framework that is able to account for the experimental observations. The key intermediate in the model is the newly observed excited state denoted $MLCT''$.

The fundamental assumption in the model is that $MLCT'$, $MLCT''$, and the ground state of $[Ru(phen)_2dppz]^{2+}$ are stabilized by polar and hydrogen bond donating solute/solvent interactions. Furthermore, it is postulated that the propensity for stabilization by both types of interactions occur in the following order,

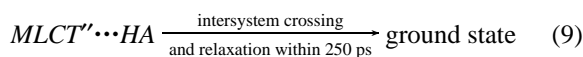
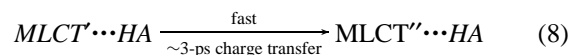
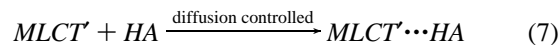


As a rough guide to the hydrogen bond accepting abilities of the ground state we can consider the ground-state basicity. The basicities of similar compounds are in the negative pK_a range (very weak bases).⁴⁸ Thus, the ground state is expected to be a weak to moderate hydrogen bond acceptor. For MLCT excited states, hydrogen bond accepting abilities are dependent on the distribution of charge in the complex. Metal complexes that feature a reduced dipyrrophenazine ligand are expected to be good hydrogen bond acceptors based on predicted charge distributions concentrated at the phenazine nitrogens. A central assumption in the model is that $MLCT''$ is the most stabilized by the hydrogen bond donating ability and polarity of the solvent.

The potential role of solvent polarity in the photophysics was recently emphasized by other authors.³⁴ With this basic element of the model in place we are able to account for the behavior of $[Ru(phen)_2dppz]^{2+}$ in different solvents. The unified model is essentially that outlined in Figure 11, but in the different environments specific kinetic limits should apply. We briefly delineate each case below.

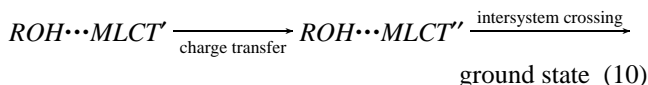
For non-hydrogen bonding, moderately polar solvents (e.g., acetonitrile), the $MLCT''$ state is sufficiently higher in energy than $MLCT'$ that the photophysics are unaffected by $MLCT''$. This is represented by the bottom scheme in Figure 11.

For mixtures of strong hydrogen bond donors HA (e.g., acetic acid) in moderately polar solvents, the observed emission is from $MLCT'$ and the HA -induced quenching is apparently diffusion controlled with minimal static quenching observed. This behavior is consistent with the following process:



Here it is assumed that HA is a sufficiently strong hydrogen bond donating species and is responsible for shifting the $MLCT'/MLCT''$ equilibrium toward $MLCT''$. Note that although $MLCT''$ is formed in this mechanism, very little emission is expected since the lifetime of $MLCT''$ (presumably at least as short as the pure water value of 250 ps) is much shorter than the lifetime of $MLCT'$, i.e. $((0.6 \mu\text{s})^{-1} + k_{\text{diff}})^{-1}$.

A quite different case is the situation in aliphatic alcohols, where the solvent is moderately hydrogen bond donating and moderately polar.³⁴ The results in these environments are consistent with the situation represented in eq 10.



Here, $MLCT'$ emission is the predominant emission since the $MLCT'/MLCT''$ equilibrium favors the $MLCT'$ form. Radiationless decay occurs through thermal activation of $MLCT''$.

The situation in acetonitrile/water mixtures is particularly complex. As water is added to acetonitrile the $MLCT'$ emission is quenched, but the effective rate of quenching is much less than diffusion controlled.³⁵ In addition, the dependence of quenching rate on H_2O concentration does not give a linear Stern–Volmer plot,³⁴ suggesting that the quenching mechanism is much more complex than simple bimolecular quenching.

In fact, $[Ru(phen)_2dppz]^{2+}$ -emission quenching by H_2O is more than three orders of magnitude less efficient than that of acetic acid at low concentrations.³⁵ Yet at high concentrations H_2O is extremely effective as a quencher. This behavior can be easily explained when both solvent polarity and hydrogen bonding are taken into account. At low to moderate concentrations of H_2O , the observed quenching by H_2O in acetonitrile is consistent with the moderate hydrogen bond donating ability of H_2O compared to acetic acid, where the observed quenching is diffusion controlled. Thus, in dilute water/acetonitrile mixtures the $MLCT'/MLCT''$ equilibrium favors $MLCT'$. The kinetics of quenching are analogous to that observed in alcohols. In striking contrast, at higher H_2O concentrations, the increase in solvent polarity is apparently capable of shifting the equilibrium toward $MLCT''$. Given a high enough concentration to shift the equilibrium in favor of $MLCT''$, there is sufficient H_2O present in the first solvent shell to allow for very rapid $MLCT'$ emission quenching. Consequently, both solvent polarity and hydrogen bond donating ability must be taken into account for water/acetonitrile mixed solvent systems.

Conclusions

In summary, the light-switch mechanism involves two steps, namely $MLCT' \rightarrow MLCT''$ interconversion and $MLCT''$ radia-

(47) Kober, E. M.; Caspar, J. V.; Lumpkin, R. S.; Meyer, T. J. *J. Phys. Chem.* **1986**, *90*, 3722–3734.

(48) Vos, J. G. *Polyhedron* **1992**, *11*, 2285–2299.

tionless decay. $MLCT'$ denotes a MLCT-emitting form which is the dominant MLCT form of $[\text{Ru}(\text{phen})_2\text{dppz}]^{2+}$ in pure acetonitrile, and is the initially formed MLCT form in other solvents. We have estimated the quantum yield of the $MLCT'$ emission in water by using time-resolved absorption and emission spectroscopies. The extraordinarily small quantum yield of the $MLCT'$ emission in water can be attributed to rapid ($\tau \approx 3$ ps) $MLCT' \rightarrow MLCT''$ interconversion, where $MLCT''$ denotes a previously unobserved emissive state. The low quantum yield of $MLCT''$ is largely a consequence of its rapid radiationless decay ($\tau \approx 250$ ps). We postulate the extraordinarily rapid radiationless decay rate for $MLCT''$ is driven by differential hydrogen bonding between the ground and excited states.

Interpreting the photophysics of $[\text{Ru}(\text{phen})_2\text{dppz}]^{2+}$ in a broad range of solvent environments reveals the significance of both the polarity and hydrogen bond donating ability of the solvent.

We propose the existence of a novel MLCT state that dramatically influences $[\text{Ru}(\text{phen})_2\text{dppz}]^{2+}$ emission properties. Significantly, the interplay between select MLCT states, distinguished by their distribution of charge on the ligand framework, has been shown to be an extremely sensitive probe of the local solvent.

Acknowledgment. This work was supported by the Department of Energy, Office of Basic Energy Science, Division of Chemical Science, the National Institutes of Health (GM33309), and the National Science Foundation. E.J.C.O. and M.R.A. were NIH NRSA trainees. A.H. thanks the Swiss National Science Foundation and E.D.A.S. thanks the American Cancer Society for postdoctoral fellowships. We would like to thank Morton Hoffman and Thomas Meyer for helpful discussions and Catherine Murphy for making a useful preprint available.

JA971151D